Acta Cryst. (1994). D**50**, 197–201

Initial Crystallographic Analysis of a Recombinant Human Interleukin-1 Receptor Antagonist Protein

BY L. L. CLANCY, B. C. FINZEL, A. W. YEM, M. R. DEIBEL JR, N. A. STRAKALAITIS AND D. P. BRUNNER

The Upjohn Company, Kalamazoo, Michigan 49001, *USA*

R. M. SWEET

Biology Department, Brookhaven National Laboratory, Upton, New York 11973, *USA*

AND H. M. EINSPAHR*

The Upjohn Company, Kalamazoo, Michigan 49001, *USA*

(*Received* 22 *April* 1993; *accepted* 6 *September* 1993)

Abstract

We report the crystallization of samples of a recombinant preparation of human interleukin-1 receptor antagonist protein (IRAP) and solution of the crystal structure by isomorphous replacement methods. Crystals were obtained by the hanging-drop vapor-diffusion method at 277 K from solutions of PEG 4000 containing sodium chloride, dithiothreitol and PIPES [sodium piperazione-*N*,*N*′-bis(2-ethanesulfonate)] buffer at pH 7.0. Crystals appear within about a week and grow as truncated tetragonal bipyramids to 0.3–0.6 mm on an edge. X-ray diffraction data from these crystals specify space group $P4_32_12$ and unit-cell dimensions of $a = b = 72.35\ (26)$, $c = 114.7\ (8)$ Å and $Z = 16$ (two molecules per asymmetric unit). Fresh crystals diffract to about 2.3 Å resolution. The search for heavy-atom derivatives has produced two, potassium gold cyanide and trimethyl lead chloride, as same-site, single-site derivatives. Inspection of an electron-density map at 4 Å resolution calculated with these derivatives confirms that the IRAP molecule is a member of the interleukin-1 structural family.

The interleukin-1 (IL-1) proteins IL-1α and IL-1β are cytokines active in a variety of processes associated with the inflammatory response (Dinarello, 1992, and references therein). Cells that secrete IL-1α and IL-1β are able to influence the behavior of cells that have specific receptors for these cytokines. IL-1α and IL-1β, which are about 25% identical in amino-acid sequence, act by binding to the extracellular domains of IL-1 receptors and triggering intracellular signals (Dower, Sims, Cerretti & Bird, 1992, and references therein). Structural studies of IL-1α (Einspahr *et al.*, 1990; Graves *et al.*, 1990) and IL-1β (Finzel *et al.*, 1989; Driscoll, Gronenborn, Wingfield & Clore, 1990), have shown that they are structurally related, with both molecules sharing an architecture that includes a six-stranded β-barrel and six other β-strands arranged in a pseudo-threefold symmetric manner.

An IL-1 receptor antagonist protein (IRAP) has been discovered (Hannum *et al.*, 1990) that appears to be a third member of the IL-1 cytokine family. It possesses sequence similarities to IL-1α (18% identical) and IL-1β (26% identical) and binds competitively to IL-1 receptors, but does not elicit expected IL-1 responses. Human IRAP has been cloned from the U937 monocyte cell line, expressed in *E. coli*, and purified (Carter *et al.*, 1990). An initial structural characterization of IRAP by X-ray crystallography is presented here.

Crystallization experiments with this protein utilized the hanging-drop vapor-diffusion method at 277 K and were set up in 24-well Linbro tissue-culture plates. Protein concentrations of 40 mg ml^{-1} and precipitant solutions within the range of 18–24% (*w*/*v*) PEG 4000 in 30 m*M* sodium piperazine-*N*,*N*′-bis(2-ethanesulfonate) (PIPES) buffer, pH 7.0, including 1 m*M* dithiothreitol, 0.6 m*M* sodium azide, and a concentration of NaCl of between 200 and 400 m*M*, have produced the best crystals. Typically, each well is filled with approximately 1 ml of the precipitant solution, and a droplet of protein, mixed in a 1:1 ratio with its respective droplet solution, is suspended under a silated glass coverslip that is sealed over each well with silicone grease. Single crystals of IRAP appear within about a week and grow as truncated tetragonal bipyramids to 0.3–0.6 mm along one edge.

* Current address: Bristol-Myers Squibb Pharmaceutical Research Institute, Route 206 and Province Line Road, Princeton, New Jersey 08543-4000, USA.

©1994 International Union of Crystallography
Printed in Great Britain – all rights reserved

Table 1. *Diffraction data summary*

$R_{sym} = \sum_{hkl}\sum_{i=1}^{N}|\langle I^{hkl}\rangle - I^{hkl}_i|/\sum_{hkl}\sum_{i=1}^{N} I^{hkl}_i$. N is the number of symmetry-related reflections. For both native and derivative data, Bijvoet paris were merged as equivalent. The R_{merge} relates the difference in observed structure-factor amplitudes between native and derivative crystals for all reflections common to both data sets. $R_{merge} = \sum|F_N - F_D|/\sum F_N$. D_2 is the resolution at which the mean ratio of intensity to standard deviation ($\langle I/\sigma\rangle$) drops to 2.0. All derivative data sets were truncated at this resolution before scaling.

Crystal (data code)	Special conditions	D_2 (Å)	Unique reflections Observed	Possible	Collected	R_{sym}	R_{merge}
Native	—	2.3	55341	14143	11831	0.066	—
$KAu(CN)_2$ (Au I)	2 m*M* 28 d soak	2.7	31146	8834	8652	0.075	0.088
$(CH_3)_3PbCl$ (Pb I)	5 m*M* 18 d soak	2.4	68446	12498	10520	0.063	0.086
$KAu(CN)_2$ (Au II)	5 m*M* 18 d soak	2.5	67320	10703	9783	0.077	0.147
$(CH_3)_3PbCl$ (Pb II)	5 m*M* 20 d soak	2.45	44663	11609	9476	0.055	0.150

Table 2. *Phasing summary, figures of merit and heavy-atom parameters*

Phasing summary

Derivative data set	Unique reflections contributing to phases: Acentric reflections	Anomalous differences	Averaged lack-of-closure residuals: Acentric (°)	Anomalous (°)	R.m.s. F_H/(error)
Au I	3896*	0	41.8	—	1.99
Pb I	4042*	0	38.8	—	1.46
Au II	4060*	4043	71.9	24.9	1.77
Pb II	4114*	4095	81.2	21.3	1.33

Figure of merit with resolution

Mean resolution (Å)	11.37	7.23	5.67	4.81	4.25	3.85	3.55	3.30	Total
Reflections phased	303	465	569	664	748	804	870	938	5,361
Mean figure of merit	0.79	0.76	0.73	0.68	0.65	0.64	0.61	0.55	0.65

Maximum resolution of phased reflections (Å) 3.2

Heavy-atom parameters

Derivative	Site	Occupancy	*x*	*y*	*z*	*B* (Å²)
$KAu(CN)_2$	AU1	0.74 (1)	0.1101 (3)	0.2010 (3)	0.0964 (2)	42 (1)
$(CH_3)_3PbCl$	PB1	0.55 (1)	0.1066 (4)	0.2020 (4)	0.0953 (2)	52 (1)
$KAu(CN)_2$	AU2	1.10 (2)	0.1085 (3)	0.2019 (3)	0.0959 (2)	40 (3)
$(CH_3)_3PbCl$	PB2	0.93 (2)	0.1046 (4)	0.2020 (4)	0.0947 (2)	40 (1)

* Only reflections with measured Bijvoet pairs (I_+ and I_-) were used in phasing.

The production of IRAP crystals in support of the structure determination effort presented several challenges. In our experience, protein solutions fail to produce crystals after about six weeks even though these solutions are maintained at 277 K. Furthermore, crystals left in droplets gradually lose the ability to diffract X-rays over a period of about two months. Finally, no artificial preservation solution was found with which to mount crystals for X-ray diffraction, to harvest and preserve crystals, or to use for making heavy-atom soak solutions. Mounting solutions were prepared by harvesting spent droplets that had produced crystals, centrifuging the harvested mixtures, and using the supernatants in 5–10 μl aliquots.

A microscale procedure was developed for preparation of heavy-atom derivatives for multiple isomorphous replacement (MIR) applications. This procedure does not involve transferring crystals between solutions and does not require a special preservation solution. First, a heavy-atom reagent solution, approximately four times more concentrated than the desired initial soak concentration, is prepared in precipitant solution similar in composition to the well solution, and a crystal still in its original droplet is selected as the target for a heavy-atom soak equipment. The coverslip supporting the droplet with the target crystal is then removed from its well and equal-sized aliquots of the heavy-atom reagent and protein solution are quickly superposed on the coverslip to make a second droplet next to, but not touching, the droplet with the target crystal. The coverslip with the pair of droplets is then quickly replaced over the well to allow the new droplet to equilibrate against the well solution. After 24–48 h, the new droplet is joined to the droplet with the crystal by drawing the former into the latter with a needle. In the procedure described here, the volume

of the new droplet is made equal to the original volume of the droplet with the target crystal when the latter was first made, but similar procedures involving other proportioning schemes may be devised.

Several data sets, including the first to specify diffraction symmetry and unit-cell dimensions, were collected at 277 K at the single-crystal diffraction facility of the Biology Department of Brookhaven National Laboratory (BNL) at the National Synchrotron Light Source (NSLS). Early data-collection attempts served to alert us to problems with non-isomorphism (or perhaps polymorphism) in IRAP crystals. The unit-cell c axis length was observed to vary from crystal to crystal, ranging from 106 to 120 Å, though diffracted intensities sometimes varied unexpectedly even in crystals with nearly identical cell constants. Crystalline specimens grown from different protein preparations showed the largest variations, but in at least one instance, large differences also were shown to arise from the same crystal over a period of several weeks. All data eventually used in the structure solution were collected from a crop of crystals derived from a single batch of protein. Further analysis of this problem is postponed until completion of the refinement of this initial structure.

All diffraction data used in structure solution were collected at room temperature. Crystals were mounted at 277 K and allowed to warm in stryofoam containers over a period of 2 h, because of apparent sensitivities to rapid warming. A Siemens imaging proportional counter mounted on the 2θ arm of a P3F four-circle goniostat was used to collect X-ray diffraction data. A Siemens rotating anode X-ray source, operated at 90 mA, 50 kV and equipped with a graphite monochromator, provided Cu $K\alpha$ radiation. For most data-collection purposes, the detector was placed 15 cm from the crystal with the normal to the detector face at an angle of 20° to the incident X-ray beam, so that data from 80 to 2.3 Å resolution were intercepted by the detector face. Data were collected in discrete 0.25° rotational scans about the ω axis at goniostat χ settings of both 0 and 90°. Reduction of raw data to integrated intensities was performed with the *XENGEN* software package (Howard *et al.*, 1987). Each data set was collected from a single crystal over a period of 2–3 d. A summary of data required for the structure solution is given in Table 1.

Unit-cell dimensions for this batch of crystals are $a = b = 72.35\,(26)$ Å, $c = 114.7\,(8)$ Å. Diffraction symmetries and systematic absences ($4/mmm$; $00l$: $l \neq 4n$, $h000$: $h \neq 2n$) specify the pair of tetragonal enantiomorphic space groups $P4_12_12$ or $P4_32_12$. For two molecules per asymmetric unit ($Z = 16$), $V_m = 2.2$ Å^3 Da^{-1} (Matthews, 1968). Attempts to solve this structure by molecular replacement with search models derived from either IL-1α or IL-1β were unsuccessful, perhaps due to the presence of two molecules in the asymmetric unit.

Two heavy-atom derivatives were useful in the calculation of phases, a potassium gold cyanide derivative and trimethyl lead chloride derivative. Conditions for producing these derivatives and summaries of diffraction data collected from two crystals of each are given in Table 1. Heavy-atom binding sites were identified with the aid of the Patterson analysis program *HASSP* (Terwilliger, Kim & Eisenberg, 1987). Heavy atoms from both derivatives

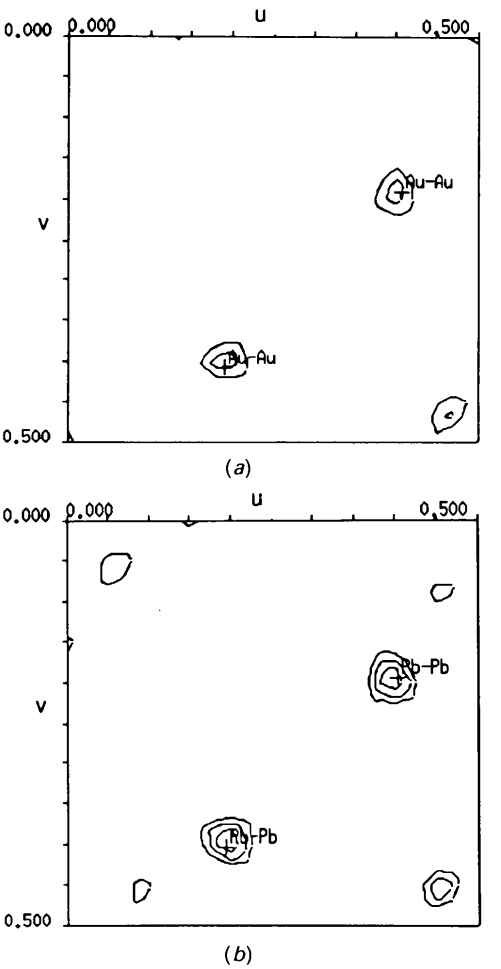

Fig. 1. Harker sections $w = 1/4$ of anomalous-difference Patterson maps computed from differences between native data and two derivative data sets, (*a*) $KAu(CN)_2$ (AU II) and (*b*) $(CH_3)_3PbCl$ (PB II). Maps are contoured at levels beginning at 2σ in successive increments of σ. The positions of peaks predicted from the refined heavy-atom positions are marked. Anomalous-difference Patterson maps computed from the two other sets of data from these derivatives lacked these consistent features, and anomalous differences from those data sets were not used in phase calculations. Maps were calculated and contoured with the aid of programs in the *XtalView* software package (McCree, 1992).

appear to occupy the same single site. Only two derivative data sets (designated Au II and Pb II) gave rise to peaks in anomalous-difference Patterson maps consistent with those observed from isomorphous differences (Fig. 1). Anomalous differences from the other two data sets (Au I and Pb I) were not used for phasing, though isomorphous differences from all four derivative data sets were included. Phases were computed by the method and programs of Terwilliger & Eisenberg (1983), and then modified by application of solvent-flattening techniques (Wang, 1985). All phase calculations were carried out in parallel for the two enantiomorphic space groups. The correct choice between enantiomorphs was resolved upon visual inspection of the density-modified maps: only the map computed under symmetry specified by space group $P4_32_12$ showed large regions of interpretable density consistent with the expected size and shape of an IL-1-like molecule. Final heavy-atom parameters are given in Table 2. While all heavy-atom position refinement was carried out to a limit of 3.2 Å resolution, maps computed with data to only 4.0 Å were significantly easier to interpret. Maps were displayed on an Evans & Sutherland PS390 graphics terminal with the program *FRODO* (Jones, 1985; Pflugrath, Saper & Quiocho, 1984), and a model was constructed. The polypeptide chains for both molecules in the asymmetric unit were easily traced from residue 8 to the C-terminus. The resulting model has not yet undergone refinement, and gives rise to a crystallographic R factor of 0.44 to 3.2 Å resolution. Backbone torsional geometry is summarized in Fig. 2. Atomic coordinates for Cα atoms will be deposited with the Protein Data Bank (Bernstein *et al.*, 1977).*

A schematic illustration of the IRAP structure resulting from our interpretation is shown in Fig. 3 where it may be compared to other IL-1 molecules. IRAP is obviously another molecule in the same

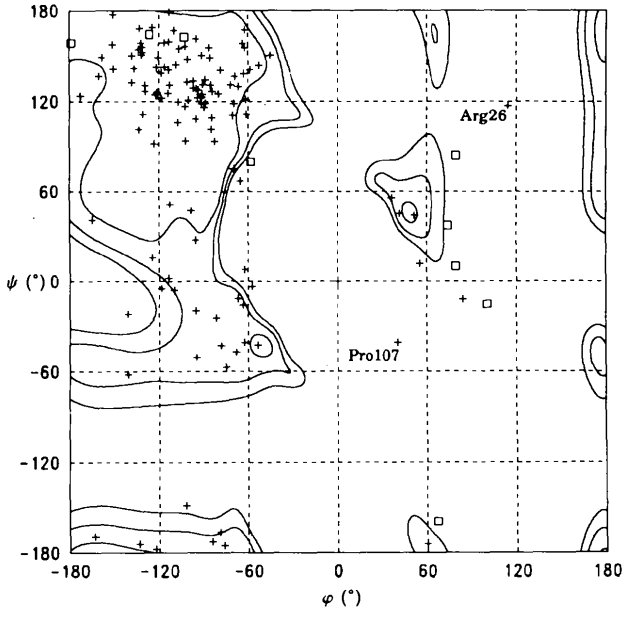

Fig. 2. A Ramachandran plot of backbone φ, ψ torsion angles for each residue in the IRAP model. The squares denote angles in glycine residues; + symbols represent non-glycine residues; Only two residues (Arg26 and Pro107) lie significantly outside regions of low energy. These residues lie in external loops where the electron density is difficult to interpret unambiguously. The model in these regions is therefore suspect.

* Atomic coordinates and structure factors have been deposited with the Protein Data Bank, Brookhaven National Laboratory (Reference: 1IRT, R1IRTSF and 1DENT, R1DENTSF). Free copies may be obtained through The Technical Editor, International Union of Crystallography, 5 Abbey Square, Chester CH1 2HU, England. Supplementary Publication No. SUP 37103). At the request of the authors, the structure factors will remain privileged until 1 November 1994. A list of deposited data is given at the end of this issue.

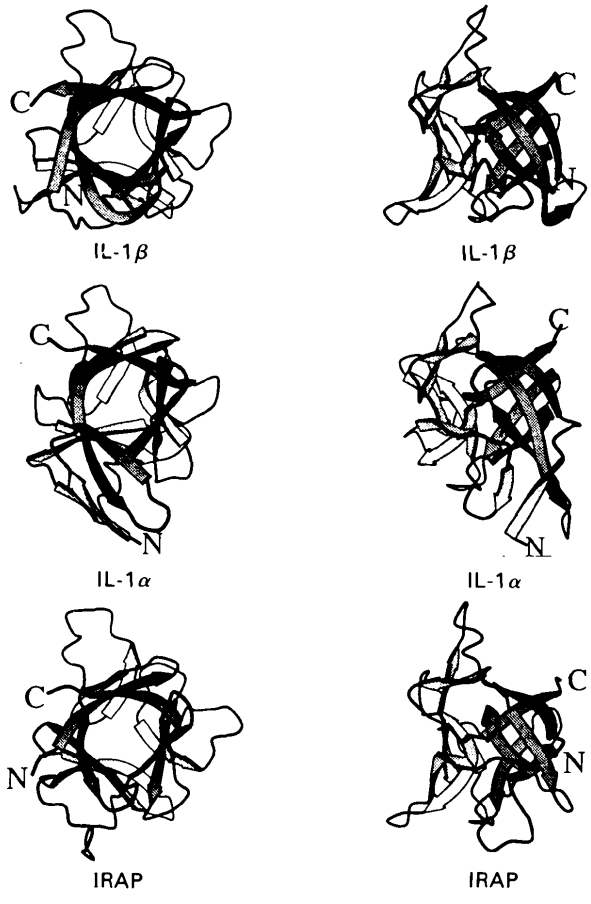

Fig. 3. Schematic illustrations of the molecular structures of IL-1β, IL-1α and IRAP. Each illustration traces the course of a polypeptide chain, with β-strand positions and directions indicated with broad arrows. The left view is down the axis of the six-stranded β-barrel (shaded darker and in front). In the right view the barrel axis is rotated to lie in the plane of the page. These illustrations were made with the *MOLSCRIPT* programs (Kraulis, 1991).

structural class. Secondary structure assignments extracted from our model agree closely with those observed by NMR for IRAP in solution (Stockman *et al.*, 1992). 12 β-strands characteristic of molecules that share this architecture are found as arranged in IL-1β, with six strands distributed around one end of a six-stranded β-barrel. Loops between strands dominate the molecular surface. IRAP and IL-1β are most different on one hemispheric face of the molecule. Loops joining strands β4 to β5, β7 to β8, and β11 to β12 in IL-1β (as described in Finzel *et al.*, 1989) adopt distinctly different conformations in IRAP, and all these loops fall onto one face of the molecule. Other loops (those joining strands β2 to β3, β3 to β4, and β5 to β6) show only small differences, while the remainder of the loops and the exposed portion of the β-barrel are nearly identical to IL-1β in backbone conformation. The backbone conformation of some, but not all, of the region of Il-1β that bears the site proposed to bind to IL-1 receptors (Labriola-Tomkins *et al.*, 1991) is conservatively replicated in IRAP, and this is equally true for IL-1α. On the other hand, none of the amino acids in positions suggested as crucial to receptor-binding efficacy in IL-1β are conserved among all three IL-1 ligand molecules.

We gratefully acknowledge the support and assistance provided by D. E. Tracey (now with BASF Bioresearch Corporation) and by colleagues in Hypersensitivity Diseases Research at Upjohn. The BNL Biology Department single-crystal diffraction facility at NSLS is supported by the Office of Health and Environmental Research of the United States Department of Energy and by an equipment grant from the National Science Foundation.

References

BERNSTEIN, F. C., KOETZLE, T. F., WILLIAMS, G. J. B., MEYER, E. F. JR, BRICE, M. D., RODGERS, J. R., KENNARD, O., SHIMANOUCHI, T. & TASUMI, K. (1977). *J. Mol. Biol.* **112**, 535–542.

CARTER, D. B., DEIBEL, M. R. JR, DUNN, C. J., TOMICH, C.-S., LABORDE, A. L., SLIGHTOM, J. L., BERGER, A. E., BIENKOWSKI, M. J., SUN, F. F., MCEWAN, R. N., HARRIS, P. K. W., YEM, A. W., WASZAK, G. A., CHOSAY, J. G., SIEU, L. C., HARDEE, M. M., ZURCHER-NEELY, H. A., REARDON, I. M., HEINRIKSON, R. L., TRUESDELL, S. E., SHELLEY, J. A., EESSALU, T. T., TAYLOR, B. M. & TRACEY, D. E. (1990). *Nature (London)*, **344**, 633–638.

DINARELLO, C. A. (1992). *Chem. Immunol. Basel Karger*, **51**, 1–32.

DOWER, S. K., SIMS, J. E., CERRETTI, D. P. & BIRD, T. A. (1992). *Chem. Immunol. Basel Karger*, **51**, 33–64.

DRISCOLL, P. C., GRONENBORN, A. M., WINGFIELD, P. T. & CLORE, G. M. (1990). *Biochemistry*, **29**, 4668–4682.

EINSPAHR, H. M., CLANCY, L. L., HOLLAND, D. R., MUCHMORE, S. W., WATENPAUGH, K. D. & FINZEL, B. C. (1990). *Current Research in Protein Chemistry*, edited by J. J. VILLAFRANCA, pp. 351–358. San Diego: Academic Press.

FINZEL, B. C., CLANCY, L. L., HOLLAND, D. R., MUCHMORE, S. W., WATENPAUGH, K. D. & EINSPAHR, H. M. (1989). *J. Mol. Biol.* **209**, 779–791.

GRAVES, B. J., HATADA, M. H., HENDRICKSON, W. A., MILLER, J. K., MADISON, V. S. & SATOW, Y. (1990). *Biochemistry*, **29**, 2679–2684.

HANNUM, C. H., WILCOX, C. J., AREND, W. P., JOSLIN, F. G., DRIPPS, D. J., HEIMDAL, P. L., ARMES, L. G., SOMMER, A., EISENBERG, S. P. & THOMPSON, R. C. (1990). *Nature (London)*, **343**, 336–340.

HOWARD, A. J., GILLILAND, G. L., FINZEL, B. C., POULOS, T. L., OHLENDORF, D. H. & SALEMME, F. R. (1987). *J. Appl. Cryst.* **20**, 383–387.

JONES, T. A. (1985). *Methods Enzymol.* **15**, 157–171.

KRAULIS, P. (1991). *J. Appl. Cryst.* **24**, 946–950.

LABRIOLA-TOMKINS, E., CHANDRAN, C., KAFFKA, K. L., BIONDI, D., GRAVES, B. J., HATADA, M., MADISON, V. S., KARAS, J., KILIAN, P. L. & JU, G. (1991). *Proc. Natl Acad. Sci. USA*, **88**, 11182–11186.

MCCREE, D. E. (1992). *J. Mol. Graphics*, **10**, 44–46.

MATTHEWS, B. W. (1968). *J. Mol. Biol.* **33**, 491–497.

PFLUGRATH, J. W., SAPER, M. A. & QUIOCHO, F. A. (1984). *Methods and Applications in Crystallographic Computing*, edited by S. R. HALL & T. ASHIDA, pp. 404–407. Oxford Univ. Press.

STOCKMAN, B. J., SCAHILL, T. A., ROY, M., ULRICH, E. L., STRAKALAITIS, N. A., BRUNNER, D. P., YEM, A. W. & DEIBEL, M. R. JR (1992). *Biochemistry*, **31**, 5237–5245.

TERWILLIGER, T. C. & EISENBERG, D. (1983). *Acta Cryst.* A**39**, 813–817.

TERWILLIGER, T. C., KIM, S. H. & EISENBERG, D. (1987). *Acta Cryst.* A**43**, 6–13.

WANG, B. C. (1985). *Methods Enzymol.* **115**, 90–112.